

Bacterial Diversity in the South Adriatic Sea during a Strong, Deep Winter Convection Year

M. Korlević,^a P. Pop Ristova,^b R. Garić,^c R. Amann,^d S. Orlić^a

Ruđer Bošković Institute, Zagreb, Croatia^a; MARUM—Centre for Marine Environmental Science, University of Bremen, Bremen, Germany^b; Institute for Marine and Coastal Research, University of Dubrovnik, Dubrovnik, Croatia^c; Max Planck Institute for Marine Microbiology, Bremen, Germany^d

The South Adriatic Sea is the deepest part of the Adriatic Sea and represents a key area for both the Adriatic Sea and the deep eastern Mediterranean. It has a role in dense water formation for the eastern Mediterranean deep circulation cell, and it represents an entry point for water masses originating from the Ionian Sea. The biodiversity and seasonality of bacterial picoplankton before, during, and after deep winter convection in the oligotrophic South Adriatic waters were assessed by combining comparative 16S rRNA sequence analysis and catalyzed reporter deposition-fluorescence *in situ* hybridization (CARD-FISH). The picoplankton communities reached their maximum abundance in the spring euphotic zone when the maximum value of the chlorophyll *a* in response to deep winter convection was recorded. The communities were dominated by *Bacteria*, while *Archaea* were a minor constituent. A seasonality of bacterial richness and diversity was observed, with minimum values occurring during the winter convection and spring postconvection periods and maximum values occurring under summer stratified conditions. The SAR11 clade was the main constituent of the bacterial communities and reached the maximum abundance in the euphotic zone in spring after the convection episode. *Cyanobacteria* were the second most abundant group, and their abundance strongly depended on the convection event, when minimal cyanobacterial abundance was observed. In spring and autumn, the euphotic zone was characterized by *Bacteroidetes* and *Gammaproteobacteria*. *Bacteroidetes* clades NS2b, NS4, and NS5 and the gamma-proteobacterial SAR86 clade were detected to co-occur with phytoplankton blooms. The SAR324, SAR202, and SAR406 clades were present in the deep layer, exhibiting different seasonal variations in abundance. Overall, our data demonstrate that the abundances of particular bacterial clades and the overall bacterial richness and diversity are greatly impacted by strong winter convection.

The Adriatic Sea is a semienclosed basin in the northeastern Mediterranean Sea. The South Adriatic Pit (SAP), the deepest part of the Adriatic Sea (maximum depth, 1,200 m), represents a key area for both the Adriatic Sea and the entire eastern Mediterranean basin. The role of the Adriatic as a source of dense water and the engine driving the eastern Mediterranean deep circulation cell is well-known (1). Open-ocean winter convection is responsible for the production of dense water, generating a mixture of the less saline waters from the Adriatic Sea with the more saline and warmer waters originating from the Ionian Sea (2). The circulation in the South Adriatic is characterized by the cyclonic South Adriatic Gyre (SAG) (Fig. 1). The East Adriatic Current (EAC), which brings warmer and more saline waters from the Ionian Sea and the Levantine Basin, and the West Adriatic Current (WAC), which transports less saline waters out of the Adriatic along the western border, characterize the cyclonic surface circulation (3). The Levantine intermediate water (LIW) and Ionian surface water (ISW) flow into the Adriatic along the South Adriatic eastern border, making this part of the Adriatic the entry point for water masses. The impact of LIW inflow on the biogeochemical cycles in the Adriatic Sea is substantial, and the fluctuation of a number of physical, chemical, and biological parameters in the Adriatic Sea has been attributed to the LIW ingression (4, 5). However, very little is known about if and how the inflow of LIW impacts the diversity and structure of picoplankton communities on a seasonal basis.

In oceanic oligotrophic waters, the temporal dynamics of prokaryotic communities were mainly described from sites used for time-series studies, which often focused exclusively on the SAR11 clade (6–8). Only a few studies describing the temporal changes in

bacterial and archaeal communities in the Mediterranean Sea have been conveyed to date (9, 10). Studies describing Adriatic picoplankton diversity mainly focused on coastal waters (11, 12). In addition, temporal studies were exclusively done in the northern coastal waters (13–16). Deep winter convective mixing was shown to shape the community structure via the transport of nutrients, i.e., phosphorus and nitrogen, to the euphotic zone, consequently triggering blooms of photosynthetic microorganisms in early spring (17). For the southern part of the Adriatic, total prokaryotic picoplankton abundances were determined during the winter convection episode in 2008, but no diversity estimation was provided (18, 19). Also, several studies have reported on seasonal changes in picoplankton heterotrophic production and bacterial community metabolic capacity, suggesting the importance and influence of the deep convection event intensity on the annual cycle and productivity of this area (20, 21). In the 2011–2012 win-

Received 15 October 2014 Accepted 18 December 2014

Accepted manuscript posted online 29 December 2014

Citation Korlević M, Pop Ristova P, Garić R, Amann R, Orlić S. 2015. Bacterial diversity in the South Adriatic Sea during a strong, deep winter convection year. *Appl Environ Microbiol* 81:1715–1726. doi:10.1128/AEM.03410-14.

Editor: J. E. Kostka

Address correspondence to S. Orlić, sandi.orlic@irb.hr.

Supplemental material for this article may be found at <http://dx.doi.org/10.1128/AEM.03410-14>.

Copyright © 2015, American Society for Microbiology. All Rights Reserved. doi:10.1128/AEM.03410-14

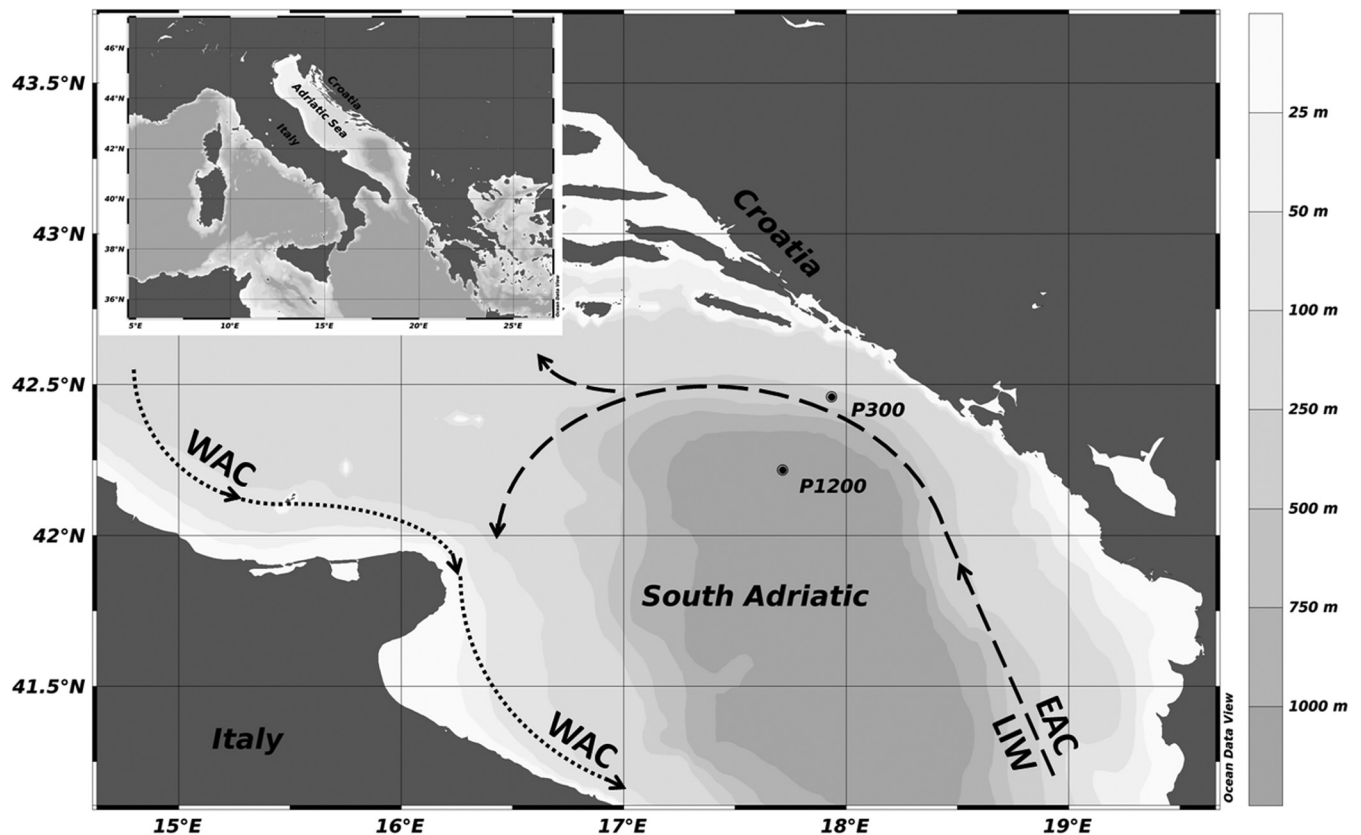


FIG 1 Study area and sampling stations in the South Adriatic Sea. EAC, east Adriatic current; WAC, west Adriatic current; LIW, Levantine intermediate water.

ter season, a strong, deep winter convection event occurred in the southern part of the Adriatic, resulting in the highest, record-breaking densities ever observed for this region (22, 23). Deep convective mixing reached down to a 600-m water depth, bringing phosphorus and nitrogen nutrients into the euphotic zone and thus triggering a bloom of photosynthetic microorganisms in early spring (21). We investigated for the first time in South Adriatic offshore waters (i) the diversity and seasonal dynamics of bacterial and archaeal communities and (ii) their response to a strong, deep winter convection event over a period of 1 year using a combination of 454 pyrosequencing of the 16S rRNA gene and catalyzed reporter deposition-fluorescence *in situ* hybridization (CARD-FISH) techniques.

MATERIALS AND METHODS

Sampling and environmental parameter estimation. Samples for bacterial and archaeal community structure analysis were taken onboard the R/V *Nasé more* on 3 October 2011, 18 February 2012, 29 March 2012, and 10 September 2012 at two stations. The stations were P-300 (42°27'32"N, 17°56'02"W), outside the SAP, and P-1200 (42°13'01"N, 17°42'50"W), inside the SAP (Fig. 1). Samples were taken with Niskin bottles at 10 depths (0 m, 10 m, 75 m, 100 m, 200 m, 400 m, 600 m, 800 m, 1,000 m, 1,200 m) at station P-1200 and 6 depths (0 m, 10 m, 75 m, 100 m, 200 m, 300 m) at station P-300. The chlorophyll *a* (Chl *a*) concentrations in samples taken on the same dates and additionally on 12 January and 30 May 2012 were determined. Seawater (500 ml) was filtered on GF/F filters (Whatman, United Kingdom). Filters were frozen at -18°C , and the Chl *a* concentration was determined by a fluorometric procedure (24). The

temperature and salinity throughout the water column were continuously recorded with an SBE25 conductivity, temperature, and depth probe (SEA-Bird Electronics Inc., USA) on the same dates that the samples for Chl *a* were taken.

454 pyrosequencing. Aliquots of 1 liter of seawater were filtered on 0.2- μm -pore-size Nuclepore polycarbonate membrane filters (Whatman, United Kingdom) with a peristaltic pump. Filters were stored in 1 ml sucrose buffer (40 mM EDTA, 50 mM Tris-HCl, 0.75 M sucrose) in liquid nitrogen and afterwards were stored at -80°C . The DNA was extracted as described by Massana et al. (25). The bacterial V1-V2 16S rRNA region was sequenced at MR DNA (Shallowater, TX, USA) using the bacterial 16S rRNA-based tag-encoded FLX amplicon pyrosequencing (bTEFAP) method (26) and Roche/454 FLX titanium instruments and reagents following the manufacturer's guidelines. Primers used for the target 16S rRNA sequence amplification were 27Fmod (5'-AGRGTTTGATCMTGG CTCAG-3') and 519Rmodbio (5'-GTNTTACNGCGGCKGCTG-3').

Sequence analysis. The standard flowgram format (SFF) files obtained were extracted using an `sff_extract` script (available at http://bioinf.comav.upv.es/sff_extract/index.html) by applying the `sff_extract -c` command, which allows sequence quality to be checked. Fasta files were split according to the bar code sequence using `mothur` software (27). Sequences containing any differences in the bar code or primer sequence were removed in the bar code splitting step. Multifasta files were processed by use of the SILVAngs pipeline (<https://www.arb-silva.de/ngs>) (28), as described by Ionescu et al. (29). Briefly, sequences were aligned against the SILVA small-subunit (SSU) rRNA SEED using the SILVA incremental aligner (SINA) (30). Sequences with low alignment quality (alignment identity of 50 and alignment score of 40 reported by SINA) were removed (as they were putative contaminations and artifacts). An

TABLE 1 Sequencing information

Sequencing characteristic	Avg \pm SD per sample	Range
Pyrotag length (bp)	412 \pm 31	200–833
No. of pyrotags	13,953 \pm 9,841	2,895–41,363
No. of classified pyrotags	13,634 \pm 9,676	2,663–40,498
No. of pyrotags with no relatives	283 \pm 229	31–1,079
No. of rejected pyrotags	36 \pm 46	2–234
No. of OTUs (97% sequence identity)	1,541 \pm 918	234–4,209
No. of singletons ^a	521 \pm 359 (33)	53–1,578 (15–48)

^a Values in parentheses are the percentage of singletons among all OTUs.

additional quality check was done by removing all sequences shorter than 200 nucleotides with more than 2% ambiguities or 2% homopolymers. Identical sequences were identified (dereplication) and clustered (operational taxonomic units [OTUs]) at 97% sequence identity using the cd-hit-est program (version 3.1.2; <http://www.bioinformatics.org/cd-hit>) (31) running in accurate mode and ignoring overhangs. The representative OTU sequence was classified by comparison with the sequences in the SILVA SSU Ref data set (release 115; <http://www.arb-silva.de>) using BLASTn software (version 2.2.22+; <http://blast.ncbi.nlm.nih.gov/Blast.cgi>) with standard settings (see Data Set S1 in the supplemental material) (32).

454 pyrosequencing of 60 samples yielded a total of 837,192 pyrotags (13,953 \pm 9,841 pyrotags, on average, per sample), with the range of the number of pyrotags in individual samples being 2,895 to 41,363. The average pyrotag length was 412 \pm 31 bp, and the minimum length was 200 bp. On average, 36 \pm 46 pyrotags were rejected in the process of quality control. The vast majority of pyrotags were successfully taxonomically assigned (13,634 \pm 9,676 pyrotags per sample). Each sample, on average, contained 1,541 \pm 918 OTUs (97% sequence identity), of which 33%, on average, were singletons (Table 1; see also Table S1 in the supplemental material). The sequencing effort applied was insufficient to determine the whole bacterial richness that could be observed in the rarefaction curves,

which did not level off even for the samples with the greatest number of pyrotags (see Fig. S1 and S2 in the supplemental material).

CARD-FISH. Water samples were fixed onboard with formaldehyde (final concentration, 2% [vol/vol]) for 24 h at 4°C. Upon arriving in the laboratory, 120 ml of water sample was filtered on a 0.2- μ m-pore-size Isopore polycarbonate membrane filter (diameter, 47 mm; GTTP Millipore, USA) and stored at -20°C . CARD-FISH using specific probes (Table 2) was performed as described by Pernthaler et al. (33), with a slight modification. Endogenous peroxidases were inactivated by incubating the filters in methanol supplemented with 0.15% H_2O_2 for 30 min. Hybridization was done in 400 μl of hybridization buffer (0.9 M NaCl, 20 mM Tris-HCl [pH 7.5], 10% [wt/vol] dextran sulfate [Sigma-Aldrich, USA], 0.01% sodium dodecyl sulfate [SDS], 1% blocking reagent [Roche, Switzerland]) supplemented with a probe-specific percentage (vol/vol) of formamide (Fluka, Germany) (Table 2) and 1.3 μl of horseradish peroxidase (HRP)-labeled probe solution (8.4 pmol μl^{-1} HRP-labeled probe in TE [Tris-EDTA] buffer; Biomers, Germany) for 2 h at 46°C. Unhybridized probes were washed by incubating the filter cuts in 50 ml of washing buffer (NaCl [at a concentration, in millimolar, specific for each probe; Table 2], 5 mM EDTA [pH 8.0], 20 mM Tris-HCl [pH 7.5], 0.01% [wt/vol] SDS) for 15 min at 48°C. After a washing step in 1 \times phosphate-buffered saline (PBS; pH 7.6, room temperature [RT], 15 min), tyramide signal amplification was performed by incubating the filter cuts in a substrate mix for 45 min at 46°C. The substrate mix was prepared by adding 1 part of Alexa 488 solution (Invitrogen, USA) to 1,000 parts of amplification buffer (0.8 \times PBS [pH 7.6], 0.08% blocking reagent, 1.6 M NaCl, 8% dextran sulfate) supplemented with freshly prepared 0.0015% H_2O_2 in 1 \times PBS. Filter cuts were washed in prewarmed (46°C) 1 \times PBS (10 min, RT). All filter cuts were counted manually (a minimum of 1,000 DAPI [4',6-diamidino-2-phenylindole] signals) on a Nikon Eclipse 50i microscope (see Data Set S2 in the supplemental material).

Data analyses. Observed richness, richness estimators (Chao1 and the abundance-based coverage estimator [ACE]), and Shannon's diversity index were calculated after normalization for the sampling effort across samples. Pyrotags corresponding to the smallest sampling effort in the data set ($n = 2,521$) were randomly resampled through rarefaction. OTUs

TABLE 2 Probes and hybridization conditions applied for CARD-FISH

Probe	Target organism	Sequence (5' \rightarrow 3')	FA concn ^a (%)	NaCl concn ^b (mM)	Reference
ARCH915	<i>Archaea</i>	GTGCTCCCGCCCAATTCTCT	35	80	55
EUB338	<i>Bacteria</i>	GCTGCCTCCCGTAGGAGT	35	80	56
EUB338-II	Supplement to EUB338	GCAGCCACCCGTAGGTGT	35	80	57
EUB338-III	Supplement to EUB338	GCTGCCACCCGTAGGTGT	35	80	57
NON338	Control	ACTCCTACGGGAGGCAGC	35	80	58
CF319a	<i>Bacteroidetes</i>	TGGTCCGTGTCTCAGTAC	35	80	59
SAR202-312R	SAR202 clade	TGTCTCAGTCCCCCTCTG	40	56	60
CYA664	<i>Cyanobacteria</i>	GGAATTCCTCTGCCCC			61
SAR406-97	SAR406 clade	CACCCGTTCCGCAAGTTA	40	56	62
ROS537	<i>Roseobacter</i>	CAACGCTAACCCCTCC	35	80	63
SAR11-152R ^c	SAR11 clade	ATTAGCACAAAGTTTCCYCGTGT	25	159	43
SAR11-441R(ori) ^c		TACAGTCATTTTCTTCCCGGAC			43
SAR11-441R(mod) ^c		TACCGTCATTTTCTTCCCGGAC			43
SAR11-487(mod) ^c		CGGACCTTCTTATTCGGG			41
SAR11-542R ^c		TCCGAACACTACGCTAGGTC			43
SAR11-732R ^c		GTCAGTAATGATCCAGAAAGYTG			43
SAR324-1412	SAR324 clade	GCCCCTGTCAACTCCCAT	35	80	41
GAM42a ^d	<i>Gammaproteobacteria</i>	GCCTTCCCACATCGTTT	35	80	64
SAR86-1245	SAR86 clade	TTAGCGTCCGTCTGTAT	35	80	65

^a FA, formamide concentration (vol/vol) in CARD-FISH hybridization buffer.

^b NaCl concentration in washing buffer.

^c A mixture of 6 probes, including an unlabeled helper, SAR11-487-h3 (5'-CGGCTGTGGCACGAAGTTAGC-3'), was used to detect the SAR11 clade.

^d Including an unlabeled competitor probe, Bet42a (5'-GCCTTCCCCTTCTGTTT-3') (64).

that were classified as chloroplasts were not taken into account. Community turnover was estimated from the resampled data by a simple accounting of the proportion of shared OTUs or taxa in two consecutive seasons or layers. Differences in richness or diversity among seasons were tested by one-way analysis of variance (ANOVA; Systat 12; Systat Software Inc., USA). The normality and homogeneity of variances were tested by the Lilliefors and Levene tests, respectively. Results found to be significant by ANOVA ($P < 0.05$) were then analyzed by *post hoc* Tukey's honestly significant difference (HSD) multiple-comparison tests to investigate which of the means were different. Differences in the relative contributions of pyrotags and the abundance of cells of SAR11, *Gammaproteobacteria*, *Bacteroidetes*, and *Cyanobacteria* (CARD-FISH-derived data) among seasons and stations were tested by two-way ANOVA (Systat 12). For the pyrotag and CARD-FISH data, only samples from the euphotic zone (<200 m) were considered, as they were retrieved from the same depths at the two stations inside and outside the SAP.

To estimate the influence of singletons (OTUs that were present as only one sequence in the whole data set), sequences with no relatives, and pooling of sequences at different taxonomic levels on bacterial diversity estimates, different data sets were constructed. Data sets containing no singletons (OTU-singl.) and only taxonomically assigned sequences (OTUannot., without the sequences with no relatives) were built. In addition, to compare the 454 pyrosequencing and CARD-FISH approaches, the relative abundances of different taxa targeted by the set of probes used in CARD-FISH (Table 2) were extracted from the 454 pyrosequencing data set and compared with the relative abundances of the same taxa detected by CARD-FISH (expressed as a percentage of the EUB338I-III signals). OTUs that were classified as chloroplasts were not taken into account. Pairwise distance matrices were calculated from the relative abundance data using the Bray-Curtis dissimilarity index (34). Dissimilarity matrices were compared by use of Pearson's product moment correlation coefficient, and significance was determined using the Mantel test followed by the Bonferroni correction. In addition, cluster analysis was performed on data sets containing the relative cell abundances detected by CARD-FISH (expressed as a percentage of the EUB338I-III signals) and the relative contribution of pyrotags taxonomically assigned to the same group. Samples were compared using the Bray-Curtis similarity coefficient, followed by a cluster analysis using the unweighted-pair group method with arithmetic means (UPGMA). All analyses were done in the R software environment (<http://www.r-project.org/>) using the package *vegan* (<http://cran.r-project.org/web/packages/vegan/index.html>) and custom scripts. Analyses testing the differences in richness among seasons and stations were done in Systat 12 (Systat Software Inc., USA).

To estimate the correlations between community and environmental parameters, Pearson's correlation coefficients were calculated. Bacterial relative abundance data derived from CARD-FISH and the relative contribution of 454 pyrosequencing pyrotags to a specific group were transformed using the Hellinger transformation, while the environmental parameters were logarithm transformed. False discovery rates (q values) based on the observed P values were calculated to ensure more stringent criteria. Correlations that matched the criteria of a P value of <0.007 , a q value of <0.1 , and an r value of >0.45 were taken into account. All correlations were performed in R using the *vegan* package, the *Hmisc* package (<http://cran.r-project.org/web/packages/Hmisc/index.html>), and Bioconductor software (<http://www.bioconductor.org/packages/release/bioc/html/qvalue.html>). The Cytoscape platform was used to visualize the network (35).

Nucleotide sequence accession numbers. The sequences obtained in this study have been submitted to the European Nucleotide Archive (ENA) under accession numbers ERS536204 to ERS536263.

RESULTS

Hydrography. Temperature stratification was observed throughout the whole year inside and outside the pit, except in winter 2012, when a deep convection episode occurred (Fig. 2a) (22).

Due to heating, in spring 2012, stratification was reestablished in a thin layer close to the surface (Fig. 2a). The intensity of the deep convection inside the pit could be discerned from the uniform temperature (13.75°C) recorded from the 10-m to the 500-m water depth (Fig. 2a). Correspondingly, during this event the salinity was uniform from the surface down to 500 to 600 m at this station, while at the station outside the pit the uniform salinity reached only to 200 m. In autumn, before the convection event, only the station outside the pit was under the influence of a saltier LIW (Fig. 2b). After the convection episode, in spring and summer, an intensification of LIW introgression was observed in the whole region and affected both stations investigated (Fig. 2b). The Chl *a* concentration varied from $<0.01 \mu\text{g liter}^{-1}$ to $4.87 \mu\text{g liter}^{-1}$. Before and after the convection episode, Chl *a* could be detected only in the euphotic zone, with the concentration maximums occurring at the deep chlorophyll maximum (DCM) between 50 and 100 m; however, during the convection, Chl *a* could be detected down to 600 m (Fig. 2c). The maximum value of Chl *a* was measured in spring 2012 at 35 m inside the pit ($4.87 \mu\text{g liter}^{-1}$), while a much lower Chl *a* concentration maximum was detected outside the pit, at 75 m ($0.88 \mu\text{g liter}^{-1}$), in the same month (Fig. 2c).

Water mass characteristics. Three types of water layers, i.e., the euphotic zone, a deep layer, and a mixed layer, which differed in temperature (T), salinity (S), and Chl *a* concentration were identified outside and inside the pit. In autumn, a euphotic zone (depth, <100 m; T , $17.93 \pm 3.26^\circ\text{C}$; S , 38.71 ± 0.11 ; Chl *a* concentration, $>0.01 \mu\text{g liter}^{-1}$) and a deep layer (depth, >100 m; T , $13.86 \pm 0.63^\circ\text{C}$; S , 38.71 ± 0.07 ; Chl *a* concentration, $<0.01 \mu\text{g liter}^{-1}$) were observed. The winter water column, characterized by a deep winter convection that reached down to 600 m, could be divided into a mixed layer (depth, <600 m; T , $13.68 \pm 0.19^\circ\text{C}$; S , 38.67 ± 0.04 ; Chl *a* concentration, $>0.01 \mu\text{g liter}^{-1}$) and a deep layer (depth, >600 m; T , $13.48 \pm 0.17^\circ\text{C}$; S , 38.71 ± 0.01 ; Chl *a* concentration, $<0.01 \mu\text{g liter}^{-1}$). The spring water column, which was characterized when the stratification was established again, could be divided into the euphotic zone (depth, <200 m; T , $14.30 \pm 0.56^\circ\text{C}$; S , 38.77 ± 0.08 ; Chl *a* concentration, $>0.01 \mu\text{g liter}^{-1}$) and a deep layer (depth, >200 m; T , $13.61 \pm 0.24^\circ\text{C}$; S , 38.70 ± 0.03 ; Chl *a* $<0.01 \mu\text{g liter}^{-1}$). The summer water column, characterized by a strong stratification, was also defined by a euphotic zone (depth, <200 m; T , $16.07 \pm 2.69^\circ\text{C}$; S , 38.85 ± 0.07 ; Chl *a* concentration, $>0.01 \mu\text{g liter}^{-1}$) and a deep layer (depth, >200 m; T , $13.63 \pm 0.44^\circ\text{C}$; S , 38.72 ± 0.06 ; Chl *a* concentration, $<0.01 \mu\text{g liter}^{-1}$). A further detailed description of the water masses, including nutrient concentrations, is given by Najdek et al. (21). Briefly, nutrient concentrations were lower in the euphotic zone and higher in the deep layer, with the exception of those in winter, when a homogeneous nutrient distribution was observed in the mixed layer.

Seasonal bacterial variation in richness, diversity, and community turnover. Different data sets were compared using Pearson's correlation coefficient in order to determine the similarity between community structure at different taxonomic levels, as well as the influence of the removal of singletons or sequences that were not taxonomically assigned (the no-relative group). The community structure showed almost no change upon removal of singleton sequences or sequences with no relatives (see Fig. S3a in the supplemental material). In contrast, when the OTU level was compared with higher taxonomic levels (genus-phyllum), a drop

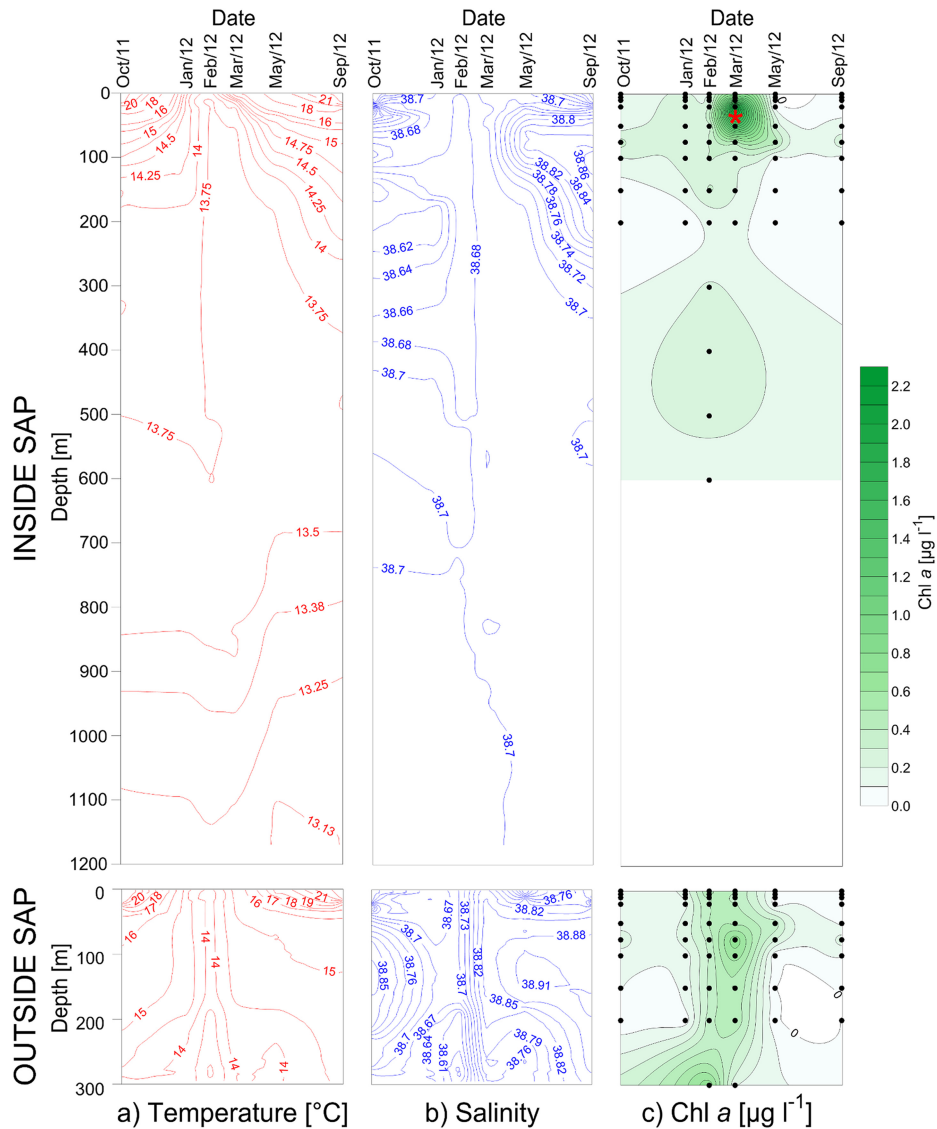


FIG 2 Vertical and seasonal distribution of temperature (a), salinity (b), and Chl *a* (c) inside and outside the SAP. Dots, sampling depths; *, Chl *a* extreme value ($4.87 \mu\text{g liter}^{-1}$) in spring 2012 at 35 m inside the pit.

in the correlation was observed (see Fig. S3a in the supplemental material).

Bacterial richness, Chao1, ACE, and Shannon diversity showed significant differences according to season ($P < 0.05$) (Fig. 3; see also Table S3 in the supplemental material). In the euphotic zone (including the mixed layer), diversity slightly increased from autumn (Chao1 = 1,121) to winter (Chao1 = 1,228) and reached the lowest numbers in spring (Chao1 = 792). Maximum values were detected in summer (Chao1 = 2,108). The pattern in the deep layer was similar, however, with the values in autumn being as high as those in summer and substantially lower than those in winter and spring.

Community turnover at different taxonomic levels was calculated to determine how much of the bacterial community is seasonally changing in the euphotic zone/mixed layer and the deep layer (see Fig. S4 in the supplemental material). The highest turnover was detected in winter and summer in the euphotic zone. The

proportion of shared OTUs in any two subsequent seasons in both the euphotic zone/mixed layer and deep layer was very low ($<1.5\%$), while at higher taxonomic levels, as expected, the proportion of shared taxa was much higher (11 to 100%). A similar pattern was observed in the euphotic zone/mixed layer and deep layer. The only difference observed between the two layers was a lower proportion of shared higher taxonomic levels (genus-phyllum) between autumn and winter in the deep layer than in the euphotic zone. In addition, the number of shared OTUs between two water layers in each season was calculated (data not shown) and also resulted in a very low number of shared OTUs ($<2\%$), reflecting the high degree of variability of microbial communities at the OTU level. A slightly higher number of shared OTUs between the euphotic zone and the deep layer was observed in spring (4.14%), reflecting the consequence of the mixing event.

Seasonal bacterial and archaeal variation. Seasonal changes in picoplankton communities were analyzed by classifying each

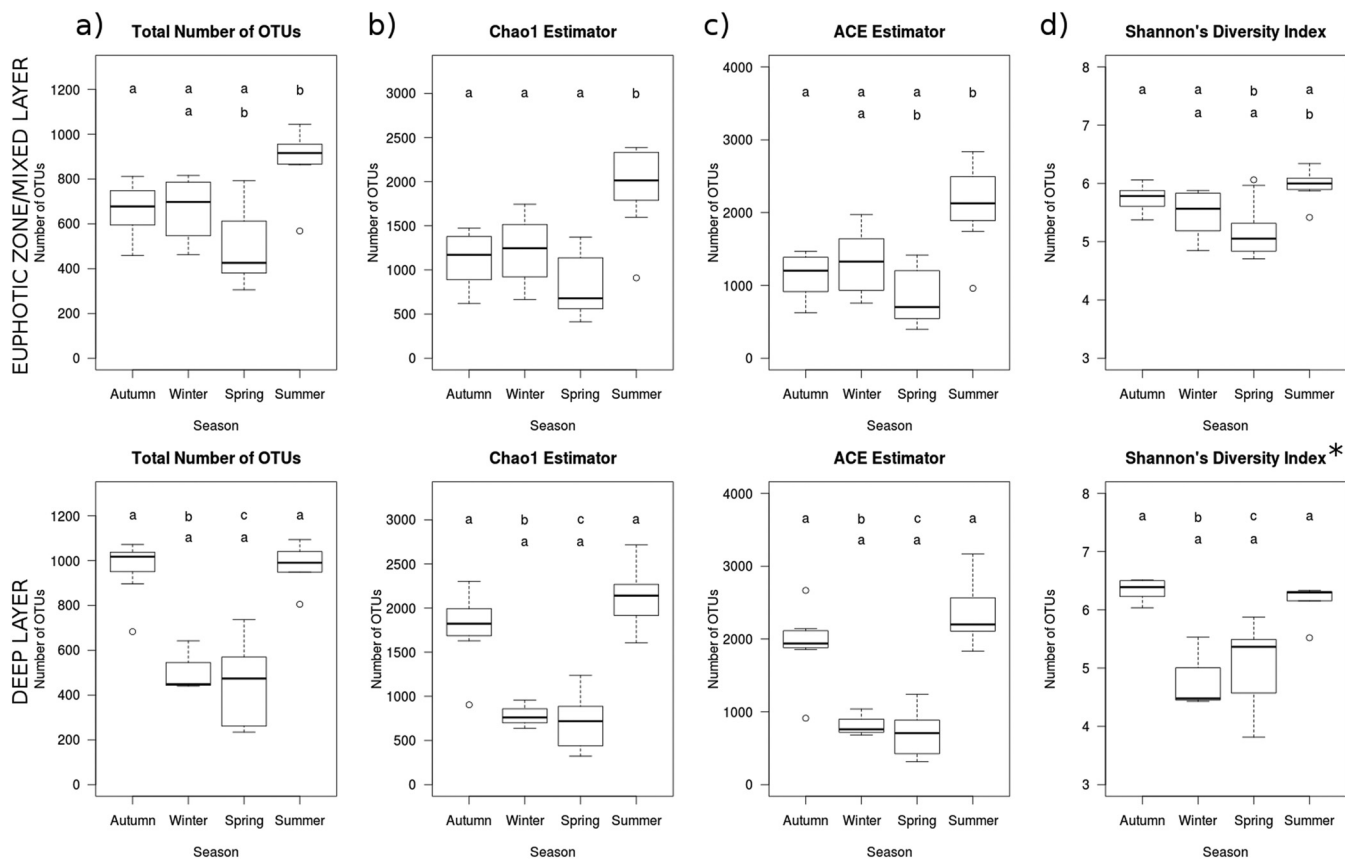


FIG 3 Total number of bacterial OTUs (a), richness predicted by the Chao1 (b) and ACE (c) estimators, and Shannon's diversity index (d) in the euphotic zone/mixed layer and deep layer of the South Adriatic Sea. The seasonal differences were tested by ANOVA. Different letters represent significant differences ($P < 0.05$, Tukey's HSD test) between seasons. *, nonhomogeneous variance.

reference OTU sequence (using the SILVA pipeline; see Table S5 in the supplemental material) and by performing the quantitative CARD-FISH analysis of major taxonomic groups (see Table S6 in the supplemental material). We used 454 pyrosequencing to get an in-depth analysis of diversity and CARD-FISH to quantify the cell numbers (absolute and relative). Two-way ANOVA of the tested phylogenetic groups (SAR11, *Gammaproteobacteria*, SAR86, *Bacteroidetes*, and *Cyanobacteria*; see Table S4 in the supplemental material) showed significant ($P < 0.05$) seasonal differences but no spatial (inside versus outside the SAP) differences (see the Results section in the supplemental material) for the CARD-FISH and 454 pyrosequencing data.

Total picoplankton cell numbers ranged from 0.94×10^5 to 8.6×10^5 cells ml^{-1} (Fig. 4a). In autumn, the cell number decreased from the euphotic zone ($3.6 \times 10^5 \text{ ml}^{-1}$) to the deep layer ($1.5 \times 10^5 \text{ ml}^{-1}$). Cell numbers were at the minimum in winter, during the deep convection (Fig. 4a). The mixed layer ($2.7 \times 10^5 \text{ ml}^{-1}$) contained higher cell numbers than the deep layer ($1.1 \times 10^5 \text{ ml}^{-1}$). In spring, characterized by a high Chl *a* concentration in the euphotic zone, the cell number reached a maximum, with a higher number being found in the euphotic zone ($4.5 \times 10^5 \text{ ml}^{-1}$) than in the deep layer ($2.0 \times 10^5 \text{ ml}^{-1}$). Summer was also characterized by a higher cell number in the euphotic zone ($3.1 \times 10^5 \text{ ml}^{-1}$) than in the deep layer ($1.8 \times 10^5 \text{ ml}^{-1}$) (Fig. 4a).

Bacteria rather than *Archaea* dominated the communities throughout the whole water column during all seasons, with

higher abundances being found in the euphotic zone/mixed layer than in the deep layer (see Fig. S9a in the supplemental material). On average, *Bacteria* comprised more than 60% of the communities, with the highest abundances being found in the euphotic zone in spring and summer (74%). The abundances of *Bacteria* in the two layers, i.e., the mixed and deep layers, were relatively more similar in winter. *Archaea* were less abundant than *Bacteria*, with higher abundances being found in the deep layer, especially in autumn (15%) and summer (13%) (Fig. 4b).

Members of the alphaproteobacterial clade SAR11 dominated the communities during the entire study period (Fig. 4c and 5). In the euphotic zone and mixed layer, they accounted for half of the picoplankton cells in autumn (50%), winter (50%), spring (48%), and summer (50%). In the deep layer, the SAR11 clade was slightly less abundant (Fig. 4c). The strong dominance of SAR11 was also reflected in the high proportion of SAR11-related pyrotags (see Fig. S6 in the supplemental material).

Cyanobacteria were characteristic of the euphotic zone (Fig. 5 and 6a). In autumn, spring, and summer, they accounted for 18%, 5.5%, and 9.1% of the communities, respectively, while in the deep layer they comprised $<1\%$ of the communities. In winter, *Cyanobacteria* accounted for $<1\%$ of the communities in the mixed layer, while in the deep layer no signal for *Cyanobacteria* was detected (Fig. 6a). We tried to derive the seasonal dynamics of the two dominant cyanobacterial genera *Synechococcus* and *Prochlorococcus* from the pyrotag frequencies. In autumn, *Synechococcus*

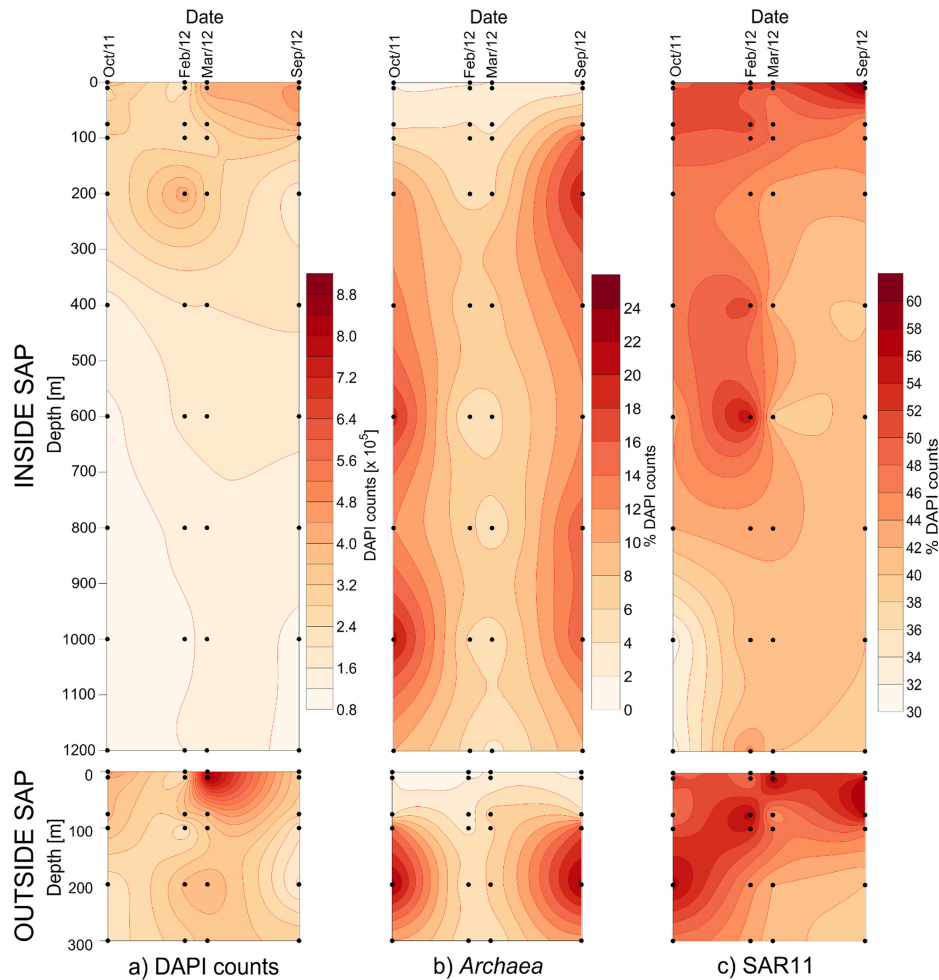


FIG 4 Vertical and seasonal distributions of total picoplankton cell (DAPI) counts (a), *Archaea* (b), and SAR11 (c) inside and outside the SAP. Dots represent sampling depths. The relative abundances of *Archaea* and SAR11 cells are represented as percentages of the DAPI counts.

occus-related pyrotags were present at a higher proportion above 75 m, while *Prochlorococcus*-related pyrotags proportionally increased with depth (see Fig. S5 in the supplemental material). In winter, almost only *Prochlorococcus*-related pyrotags were found. Spring was characterized by an approximately equal relative abundance of *Prochlorococcus*- and *Synechococcus*-related pyrotags in the euphotic zone, while in summer *Prochlorococcus*-related pyrotags were highly dominant in the deep chlorophyll maximum (DCM) layer (75 m; see Fig. S5 in the supplemental material).

CARD-FISH indicated that *Gammaproteobacteria* were prevalent in the euphotic zone in autumn, spring, and summer, accounting for 12%, 9.5%, and 7.4% of the communities, respectively, while in the deep layer they accounted for <3% of the communities, on average (Fig. 5 and 6b). During the deep convection they accounted for <3% of the communities in the mixed layer, while no signal was observed in the deep layer (Fig. 6b). The main gammaproteobacterial clade detected throughout this study was SAR86 (see Fig. S7 in the supplemental material). Members of the SAR86 clade were characteristic of the euphotic zone/mixed layer, with the highest abundance being detected in autumn and summer (4.0%), while in the deep layer they accounted for, on average, <1% of the communities (see Fig. S9c in the supplemental material).

The distribution of *Bacteroidetes* was similar to that of *Gammaproteobacteria*, with higher abundances being detected in the euphotic zone/mixed layer and with abundance peaks being detected in autumn (6%) and spring (7.5%) (Fig. 5 and 6c). Pyrotags related to the order *Flavobacteriales* were abundant, with high frequencies of clades NS2b, NS4, and NS5 being detected (see Fig. S8 in the supplemental material).

Members of the deltaproteobacterial SAR324 clade were abundant in the deep layer, with an abundance peak occurring in the summer deep-layer samples (8.0%). During the phase of stratification, they always comprised <2% of total prokaryotes in the photic layer (see Fig. S10a in the supplemental material). SAR202 clade members were characteristic of the deep layer and the winter mixed layer, while in the euphotic zone they comprised <2% of the total prokaryotes (see Fig. S10b in the supplemental material). The maximum abundance was observed in the autumn (8.7%) and winter (9.3%) deep layers. The SAR406 clade, similar to SAR324 and SAR202, was more abundant in the deep layer, especially in summer, when it accounted for 12% of the total prokaryotes (see Fig. S10c in the supplemental material).

A comparison of the CARD-FISH and 454 pyrosequencing data sets using Pearson's correlation coefficient was performed to estimate if the CARD-FISH and 454 pyrosequencing approaches

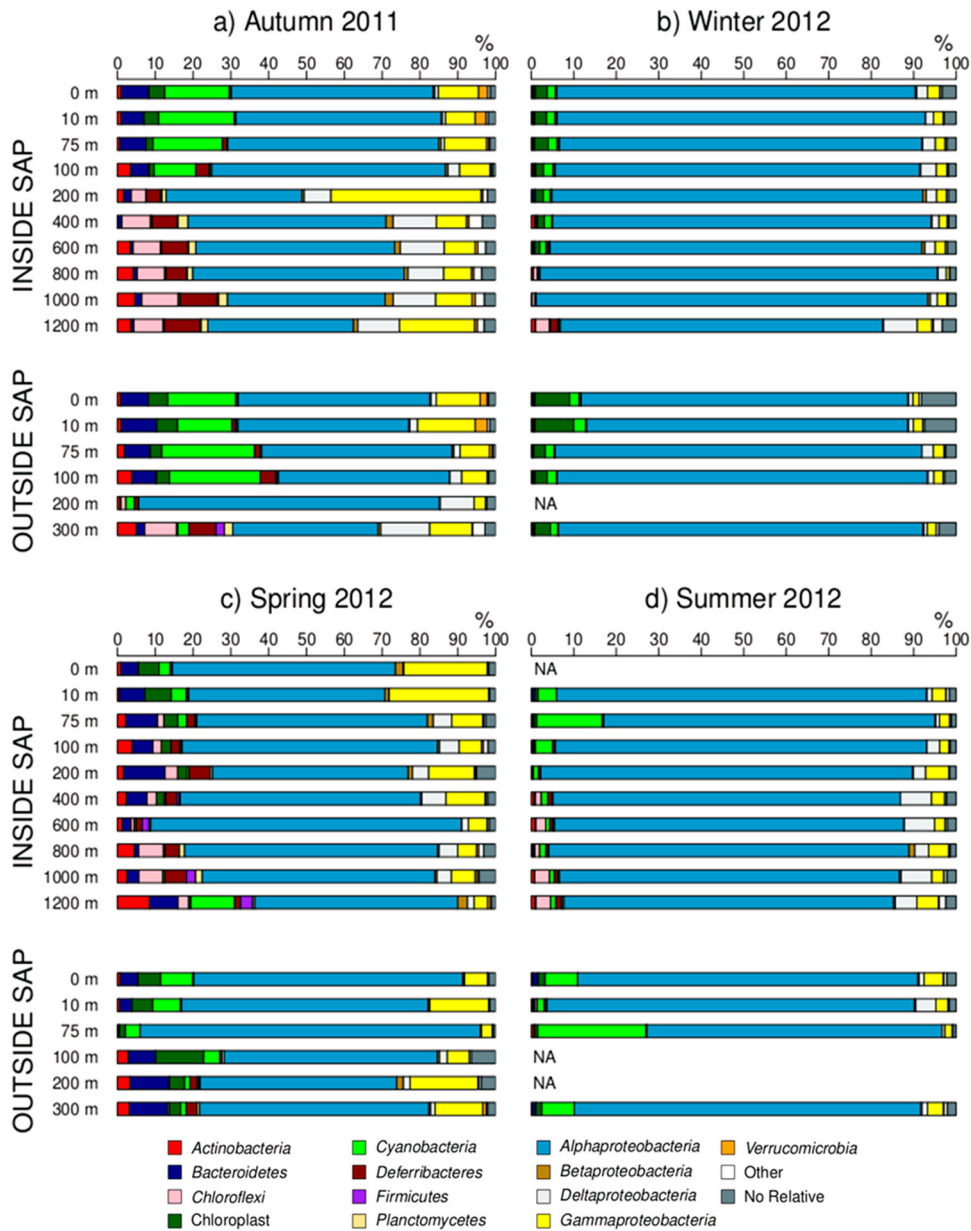


FIG 5 Taxonomic classifications and relative contribution of the most common bacterial pyrotags (>2%) inside and outside the SAP. NA, data not available.

show the same community structure (see Fig. S3b in the supplemental material). The relative abundances of different taxonomic groups detected by CARD-FISH were compared with the relative abundances of the same taxonomic groups found in the 454 pyrosequencing data set and with the different taxonomic levels of the 454 pyrosequencing data set. A weak positive correlation between the CARD-FISH and 454 pyrosequencing data set ($R = 0.21$, $P < 0.05$) was observed, indicating that the two methods show the same direction of the underlying patterns but that the bacterial structure revealed by the two methods is not the same (see Fig. S3b in the supplemental material). In addition, a cluster analysis was performed to reveal the differences in the clustering of the samples using the CARD-FISH and 454 pyrosequencing data (see Fig. S12 in the supplemental material). The dendrogram

based on the CARD-FISH data showed two clusters, one mainly containing samples from the euphotic zone and one containing samples from the deep/mixed layer. On the other hand, 454 pyrosequencing data showed the clustering of winter and summer samples in one cluster and of autumn and spring samples in the other, with an additional cluster containing samples with a high contribution of *Sphingomonadales*-related pyrotags.

DISCUSSION

In this study, we present findings on the seasonal dynamics of picoplankton communities in the South Adriatic through the whole water column over a period of 1 year in which a strong, deep convection occurred. Our results are based on a combination of two molecular techniques, the high-resolution 454 pyrosequencing

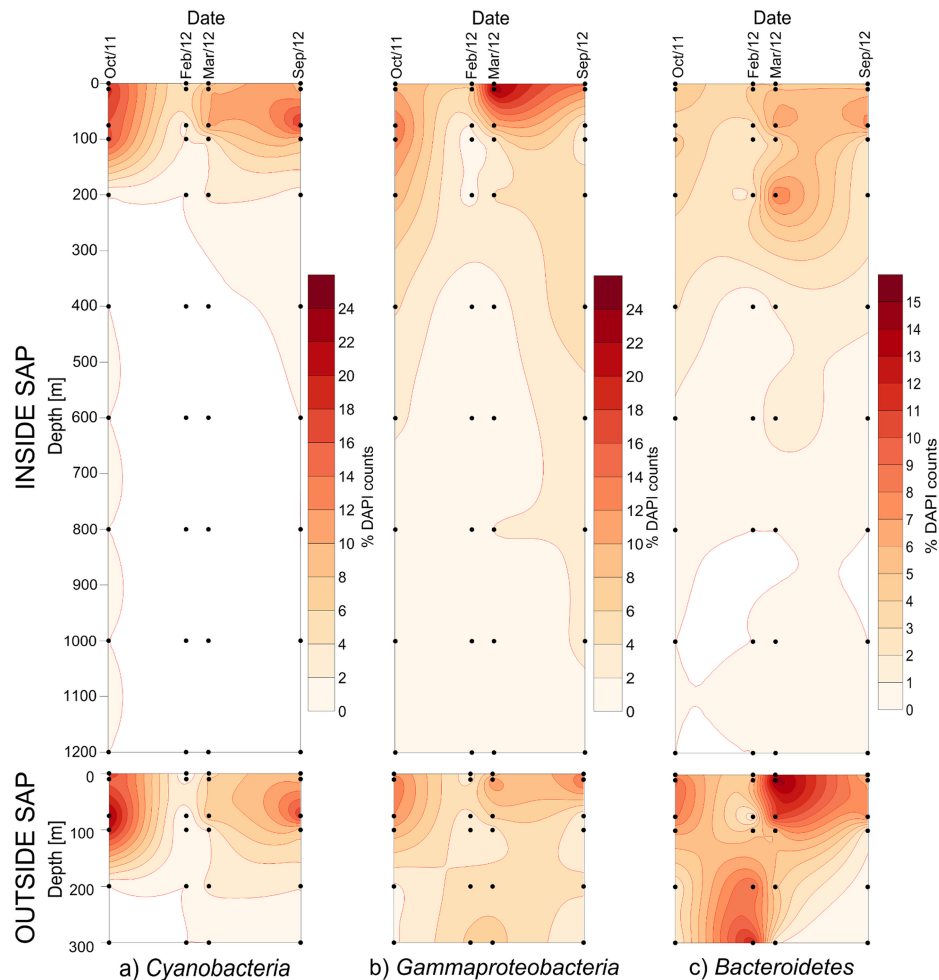


FIG 6 Vertical and seasonal distribution of *Cyanobacteria* (a), *Gammaproteobacteria* (b), and *Bacteroidetes* (c) inside and outside the SAP. Relative cell abundances are represented as percentages of the DAPI counts.

ing and the quantitative CARD-FISH techniques. Only a weakly positive correlation between the CARD-FISH and 454 pyrosequencing data was found. In addition, the CARD-FISH and 454 pyrosequencing data were used to build a cluster dendrogram that showed a different clustering of a part of the samples. The discrepancies in the compositional information obtained by 454 pyrosequencing and CARD-FISH data likely result from the distortion of 454 pyrosequencing read frequencies by PCR bias, problems with library construction, clade-specific differences in the rRNA operon number, and DNA extraction efficiency. In addition, the inactive physiological status of the cells can lead to discrepancies. Half of the picoplankton community is composed of SAR11, which has a low rRNA content, especially at greater depths, which can lead to an underestimation of SAR11 counts by CARD-FISH (36).

A deep-water convection event, typical for midlatitude ecosystems, is one of the most important factors influencing seasonal picoplankton dynamics (e.g., cell numbers, metabolic activities) in the South Adriatic (6, 7, 17). The observed convection is peculiar and stronger than that in other midlatitude systems because of the local meteorological conditions (strong winds) and hydrographic conditions needed for dense water formation (22, 23).

This strong convection event greatly influenced the distribution of different picoplankton clades not only by transporting typical deep-water clades, such as SAR324, SAR202, and SAR406, to the surface but also indirectly by supplying nutrients for phytoplankton blooms. In addition, the convection event influenced the bacterial diversity and composition in both the euphotic zone and the deep layer.

The alpha diversity of euphotic bacterial communities in the South Adriatic varied strongly according to season, with the highest abundances being detected in summer and the lowest abundances being detected in the postconvection period, i.e., spring. In the euphotic zone, the increase in richness to the summer maximum observed was different from that in western English Channel surface waters, where a winter maximum and a summer minimum were observed (37, 38), and from that in the Bermuda Atlantic Time-Series Study (BATS), where an opposite pattern was detected, with higher richness values being found in winter, during the mixing, and lower richness values being found in summer, under stratified conditions (17). The diversity minimum in spring, during the maximum productivity, could be explained by the availability of a series of new ecological niches due to the production of phytoplankton-derived organic matter, in which spe-

cialists could bloom (39). In addition, the maximum richness observed in summer could be explained by the intensification of the gyre (in summer, both stations were under the influence of LIW) that caused a stronger introgression of LIW, a possible source of new LIW-specific subclades (21, 40).

During the entire year, the euphotic zone and the mixed layer were dominated by *Bacteria*, while *Archaea* were only a minor constituent, as was found elsewhere (41, 42). SAR11 was the most abundant phylogenetic group and regularly accounted for more than 40% of the communities. A similar seasonal pattern of a postconvection SAR11 maximum was found in the northwestern Sargasso Sea (7), while in a coastal oligotrophic Mediterranean system, a higher relative abundance of SAR11 was detected in spring and summer (9). However, in both studies the relative contribution of SAR11 to the whole community was lower than that in our study. This could, however, also be attributed to the lower number of SAR11-specific probes used in these studies, as here a highly sensitive combination of six FISH probes, one helper oligonucleotide, and signal amplification via CARD-FISH was applied for the quantification of SAR11. The worldwide distribution and high annual abundance of this clade (43), supported by genomic data (44, 45), suggest that the SAR11 clade plays a major role in the oxidation of low-molecular-weight dissolved organic matter in oligotrophic systems.

The seasonality of *Cyanobacteria*, which was the second most abundant group, strongly depended on the convection event when a strong decrease in their relative abundance was observed. A similar strong decrease in *Prochlorococcus* abundances due to a seasonal deep convection, which was attributed to the selective elimination of low-light (LL)-adapted *Prochlorococcus* ecotypes incapable of coping with turbulent deep winter mixing, was observed at BATS (46). In autumn, *Synechococcus*-specific pyrotags were dominant above 75-m water depths, while below 75 m, *Prochlorococcus*-specific pyrotags were more abundant. In other seasons, only *Prochlorococcus*-specific pyrotags or the same abundance of pyrotags specific to both genera could be found at all depths (47). The increase of *Bacteroidetes* and *Gammaproteobacteria* in spring detected here is atypical of the findings for oligotrophic offshore waters (41). However, in coastal and eutrophic systems, the increase in the abundance of these two groups in spring has been linked to phytoplankton blooms and was related to the breakdown of the biomass of phytoplankton blooms (39, 48). Furthermore, it was suggested that *Bacteroidetes* are increasingly being replaced by *Gammaproteobacteria* in the postbloom period (39, 48). A similar pattern could be observed in our data in autumn and spring. The response of these groups to a phytoplankton bloom could be observed, especially in spring, when, in a postconvection period, the highest Chl *a* concentration, which was mainly attributed to *Chaetoceros* spp. and *Guinardia striata* diatom blooms, was observed (S. Ljubimir, personal communication). In coastal waters, *Ulvibacter*, *Formosa*-related, and *Polaribacter* species from the order *Flavobacteriales*, phylum *Bacteroidetes*, were found to increase in number during or shortly after a diatom bloom (39). Although *Bacteroidetes*-specific pyrotags from the South Adriatic were mainly assigned to the *Flavobacteriales*, none of the groups mentioned above were found in high numbers. Instead, the NS2b, NS4, and NS5 clades were the main *Flavobacteriales* groups, indicating that they could be better adapted to oligotrophic conditions. In the same study, *Reinekea* and SAR92 gammaproteobacterial groups were found to increase

in number after the diatom bloom and as a response to algal decay (39). Similar to the findings for the *Bacteroidetes* groups, no *Reinekea* species- or SAR92-specific pyrotags were observed in high proportions, but instead, SAR86 dominated the *Gammaproteobacteria*, indicating that SAR86 is an analog of *Reinekea* spp. and SAR92 in oligotrophic offshore waters.

The deep-layer samples showed a higher relative abundance of *Archaea*, especially in autumn and summer, than the euphotic and mixed layers. A similar abundance of *Archaea* was observed in the Atlantic mesopelagic waters (41, 49) and eastern Mediterranean deep waters (50). The greater abundance of *Archaea* in the deep layer in autumn and summer points to a response of *Archaea* to processes in the euphotic zone (51). In winter at 800 m and 1,000 m and in spring at 600 m, an unexpected dominance of *Sphingomonadales*-related pyrotags almost completely belonging to a single genus (*Sphingobium*) was observed. Blooms of a single species from the order *Sphingomonadales* have previously been reported in a coastal lagoon and co-occurred with a bloom of filamentous cyanobacteria (52). The SAR202 clade exhibits an abundance pattern similar to that of *Archaea*, being more abundant in the deep layer in autumn and summer but not in winter, when it is uniformly distributed through the water column (41, 53). The SAR406 clade comprised ~6% of the deep-layer communities throughout the year, with the exception of summer, when its abundance increased to more than 10%. The deltaproteobacterial SAR324 clade, like the SAR406 clade, peaked in the deep layer in summer, with a secondary peak occurring in the winter mixed layer (41). In the same study, patchy distributions of SAR406 along the Atlantic transect that were explained by a possible natural variation due to seasonality were observed (41). The same explanation could be applied to explain the summer seasonal peak of SAR406 in our study.

The environmental parameters measured did not reveal any clear insight into the factors that shape the bacterial distribution in the South Adriatic (see the Results section in the supplemental material). Of all abundant taxa, only the *Deferribacteres* significantly correlated with nitrate concentrations, as was previously found in the western English Channel, but apart from that, the presence of bacterial groups mainly correlated with the presence of other bacterial groups, indicating the difficulties in explaining bacterial distributions and dynamics using correlation methods, especially in cases of seasonal sampling campaigns (38, 54).

Overall, we showed in this study that the strong winter convection of 2012 had profound consequences for the bacterial and archaeal picoplankton communities of the South Adriatic Sea with respect to species richness, species diversity, and the abundances of different phylogenetic groups. The convection episodes are obviously changing the biogeochemistry and microbiology of the whole Adriatic. In the future, high-frequency sampling might reveal further details on the surprisingly dynamic succession of picoplankton clades in oligotrophic offshore waters.

ACKNOWLEDGMENTS

Financial support was provided by the Croatian Science Foundation through the BABAS project. Further support came from the German Academic Exchange Service DAAD (to S.O.). M.K. and S.O. are grateful for the support of COST action ES1103. P.P.R. thanks DFG, through Emmy Noether group no. BU 2606/1-1, for additional personal funds.

We thank the captain and crew of the R/V *Náše more*, colleagues from the Institute for Marine and Coastal Research, University of Dubrovnik,

and colleagues from the Laboratory for Marine Microbial Ecology, Center for Marine Research, Ruđer Bošković Institute, Rovinj, Croatia, for help during sampling and technical support. M.K. is grateful for fruitful discussions with colleagues from the Max Planck Institute for Marine Microbiology, Bremen, Germany, in particular, Bernhard Fuchs for advice on CARD-FISH and Renzo Kottmann for support during the COST-STSM.

REFERENCES

- Ovchinnikov IM, Zats VI, Krivosheya VG, Udodov AI. 1985. A forming of deep eastern Mediterranean water in the Adriatic Sea. *Okeanologia* 25:911–917. (In Russian.)
- Gačić M, Civitarese G. 2012. Introductory notes on the South Adriatic oceanography. *Cont Shelf Res* 44:2–4. <http://dx.doi.org/10.1016/j.csr.2012.02.019>.
- Zore M. 1956. On the gradient currents in the Adriatic Sea. *Acta Adriat* 8:1–38.
- Batistić M, Kršinić F, Jasprica N, Carić M, Viličić D, Lučić D. 2004. Gelatinous invertebrate zooplankton of the South Adriatic: species composition and vertical distribution. *J Plankton Res* 26:459–474. <http://dx.doi.org/10.1093/plankt/fbh043>.
- Civitarese G, Gačić M, Lipizer M, Eusebi Borzelli GL. 2010. On the impact of the Bimodal Oscillating System (BiOS) on the biogeochemistry and biology of the Adriatic and Ionian Seas (eastern Mediterranean). *Biogeosciences* 7:3987–3997. <http://dx.doi.org/10.5194/bg-7-3987-2010>.
- Morris RM, Vergin KL, Cho J-C, Rappe MS, Carlson CA, Giovannoni SJ. 2005. Temporal and spatial response of bacterioplankton lineages to annual convective overturn at the Bermuda Atlantic time-series study site. *Limnol Oceanogr* 50:1687–1696. <http://dx.doi.org/10.4319/lo.2005.50.5.1687>.
- Carlson CA, Morris R, Parsons R, Treusch AH, Giovannoni SJ, Vergin K. 2009. Seasonal dynamics of SAR11 populations in the euphotic and mesopelagic zones of the northwestern Sargasso Sea. *ISME J* 3:283–295. <http://dx.doi.org/10.1038/ismej.2008.117>.
- Eiler A, Hayakawa DH, Church MJ, Karl DM, Rappé MS. 2009. Dynamics of the SAR11 bacterioplankton lineage in relation to environmental conditions in the oligotrophic North Pacific subtropical gyre. *Environ Microbiol* 11:2291–2300. <http://dx.doi.org/10.1111/j.1462-2920.2009.01954.x>.
- Alonso-Sáez L, Balagué V, Sà EL, Sánchez O, González JM, Pinhassi J, Massana R, Pernthaler J, Pedrós-Alió C, Gasol JM. 2007. Seasonality in bacterial diversity in north-west Mediterranean coastal waters: assessment through clone libraries, fingerprinting and FISH. *FEMS Microbiol Ecol* 60:98–112. <http://dx.doi.org/10.1111/j.1574-6941.2006.00276.x>.
- Diez-Vives C, Gasol JM, Acinas SG. 2012. Evaluation of marine Bacteroidetes-specific primers for microbial diversity and dynamics studies. *Microb Ecol* 64:1047–1055. <http://dx.doi.org/10.1007/s00248-012-0087-x>.
- Manti A, Boi P, Semprucci F, Cataudella R, Papa S. 2012. Picoplankton community composition by CARD-FISH and flow cytometric techniques: a preliminary study in central Adriatic Sea water. *Int J Oceanogr* 2012: 909718. <http://dx.doi.org/10.1155/2012/909718>.
- Quero GM, Luna GM. 2014. Diversity of rare and abundant bacteria in surface waters of the southern Adriatic Sea. *Mar Genomics* 17:9–15. <http://dx.doi.org/10.1016/j.margen.2014.04.002>.
- Celussi M, Cataletto B. 2007. Annual dynamics of bacterioplankton assemblages in the Gulf of Trieste (northern Adriatic Sea). *Gene* 406:113–123. <http://dx.doi.org/10.1016/j.gene.2007.07.010>.
- Celussi M, Bussani A, Cataletto B, Del Negro P. 2011. Assemblages' structure and activity of bacterioplankton in northern Adriatic Sea surface waters: a 3-year case study. *FEMS Microbiol Ecol* 75:77–88. <http://dx.doi.org/10.1111/j.1574-6941.2010.00997.x>.
- Šilović T, Balagué V, Orlić S, Pedrós-Alió C. 2012. Picoplankton seasonal variation and community structure in the northeast Adriatic coastal zone. *FEMS Microbiol Ecol* 82:678–691. <http://dx.doi.org/10.1111/j.1574-6941.2012.01438.x>.
- Tinta T, Vojvoda J, Mozetič P, Talaber I, Vodopivec M, Malfatti F, Turk V. 5 June 2014. Bacterial community shift is induced by dynamic environmental parameters in a changing coastal ecosystem (northern Adriatic, northeastern Mediterranean Sea)—a 2-year time-series study. *Environ Microbiol*. <http://dx.doi.org/10.1111/1462-2920.12519>.
- Vergin K, Done B, Carlson C, Giovannoni S. 2013. Spatiotemporal distributions of rare bacterioplankton populations indicate adaptive strategies in the oligotrophic ocean. *Aquat Microb Ecol* 71:1–13. <http://dx.doi.org/10.3354/ame01661>.
- Batistić M, Jasprica N, Carić M, Čalić M, Kovačević V, Garić R, Njire J, Mikuš J, Bobanović-Čolić S. 2012. Biological evidence of a winter convection event in the South Adriatic: a phytoplankton maximum in the aphotic zone. *Cont Shelf Res* 44:57–71. <http://dx.doi.org/10.1016/j.csr.2011.01.004>.
- Cerino F, Bernardi Aubry F, Coppola J, La Ferla R, Maimone G, Socal G, Totti C. 2012. Spatial and temporal variability of pico-, nano- and microphytoplankton in the offshore waters of the southern Adriatic Sea (Mediterranean Sea). *Cont Shelf Res* 44:94–105. <http://dx.doi.org/10.1016/j.csr.2011.06.006>.
- Azzaro M, La Ferla R, Maimone G, Monticelli LS, Zaccone R, Civitarese G. 2012. Prokaryotic dynamics and heterotrophic metabolism in a deep convection site of eastern Mediterranean Sea (the Southern Adriatic Pit). *Cont Shelf Res* 44:106–118. <http://dx.doi.org/10.1016/j.csr.2011.07.011>.
- Najdek M, Paliaga P, Šilović T, Batistić M, Garić R, Supić N, Ivančić I, Ljubimir S, Korlević M, Jasprica N, Hrustić E, Dupčić-Radić I, Blažina M, Orlić S. 2014. Picoplankton community structure before, during and after convection event in the offshore waters of the southern Adriatic Sea. *Biogeosciences* 11:2645–2659. <http://dx.doi.org/10.5194/bg-11-2645-2014>.
- Mihanović H, Vilibić I, Carniel S, Tudor M, Russo A, Bergamasco A, Bubić N, Ljubešić Z, Viličić D, Boldrin A, Malačić V, Celio M, Comici C, Raicich F. 2013. Exceptional dense water formation on the Adriatic shelf in the winter of 2012. *Ocean Sci* 9:561–572. <http://dx.doi.org/10.5194/os-9-561-2013>.
- Bensi M, Cardin V, Rubino A, Notarstefano G, Poulain PM. 2013. Effects of winter convection on the deep layer of the southern Adriatic Sea in 2012. *J Geophys Res Ocean* 118:6064–6075. <http://dx.doi.org/10.1002/2013JC009432>.
- Holm-Hansen O, Lorenzen CJ, Holmes RW, Strickland JDH. 1965. Fluorometric determination of chlorophyll. *ICES J Mar Sci* 30:3–15. <http://dx.doi.org/10.1093/icesjms/30.1.3>.
- Massana R, Murray AE, Preston CM, Delong EF. 1997. Vertical distribution and phylogenetic characterization of marine planktonic archaea in the Santa Barbara Channel. *Appl Environ Microbiol* 63:50–56.
- Dowd SE, Sun Y, Wolcott RD, Domingo A, Carroll JA. 2008. Bacterial tag-encoded FLX amplicon pyrosequencing (bTEFAP) for microbiome studies: bacterial diversity in the ileum of newly weaned Salmonella-infected pigs. *Foodborne Pathog Dis* 5:459–472. <http://dx.doi.org/10.1089/fpd.2008.0107>.
- Schloss PD, Westcott SL, Ryabin T, Hall JR, Hartmann M, Hollister EB, Lesniewski RA, Oakley BB, Parks DH, Robinson CJ, Sahl JW, Stres B, Thallinger GG, Van Horn DJ, Weber CF. 2009. Introducing mothur: open-source, platform-independent, community-supported software for describing and comparing microbial communities. *Appl Environ Microbiol* 75:7537–7541. <http://dx.doi.org/10.1128/AEM.01541-09>.
- Quast C, Pruesse E, Yilmaz P, Gerken J, Schwaer T, Yarza P, Peplies J, Glöckner FO. 2013. The SILVA ribosomal RNA gene database project: improved data processing and web-based tools. *Nucleic Acids Res* 41: D590–D596. <http://dx.doi.org/10.1093/nar/gks1219>.
- Ionescu D, Siebert C, Polerecky L, Munwes YY, Lott C, Häusler S, Bizić-Ionescu M, Quast C, Peplies J, Glöckner FO, Ramette A, Rödlger T, Dittmar T, Oren A, Geyer S, Stärk H-J, Sauter M, Licha T, Laronne JB, de Beer D. 2012. Microbial and chemical characterization of under-water fresh water springs in the Dead Sea. *PLoS One* 7:e38319. <http://dx.doi.org/10.1371/journal.pone.0038319>.
- Pruesse E, Peplies J, Glöckner FO. 2012. SINA: accurate high-throughput multiple sequence alignment of ribosomal RNA genes. *Bioinformatics* 28: 1823–1829. <http://dx.doi.org/10.1093/bioinformatics/bts252>.
- Li W, Godzik A. 2006. Cd-hit: a fast program for clustering and comparing large sets of protein or nucleotide sequences. *Bioinformatics* 22:1658–1659. <http://dx.doi.org/10.1093/bioinformatics/btl158>.
- Camacho C, Coulouris G, Avagyan V, Ma N, Papadopoulos J, Bealer K, Madden TL. 2009. BLAST+: architecture and applications. *BMC Bioinformatics* 10:421. <http://dx.doi.org/10.1186/1471-2105-10-421>.
- Pernthaler A, Pernthaler J, Amann R. 2002. Fluorescence in situ hybridization and catalyzed reporter deposition for the identification of marine bacteria. *Appl Environ Microbiol* 68:3094–3101. <http://dx.doi.org/10.1128/AEM.68.6.3094-3101.2002>.
- Bray JR, Curtis JT. 1957. An ordination of the upland forest communities

- of southern Wisconsin. *Ecol Monogr* 27:325. <http://dx.doi.org/10.2307/1942268>.
35. Shannon P, Markiel A, Ozier O, Baliga NS, Wang JT, Ramage D, Amin N, Schwikowski B, Ideker T. 2003. Cytoscape: a software environment for integrated models of biomolecular interaction networks. *Genome Res* 13: 2498–2504. <http://dx.doi.org/10.1101/gr.1239303>.
 36. De Corte D, Sintes E, Yokokawa T, Herndl GJ. 2013. Comparison between MICRO-CARD-FISH and 16S rRNA gene clone libraries to assess the active versus total bacterial community in the coastal Arctic. *Environ Microbiol Rep* 5:272–281. <http://dx.doi.org/10.1111/1758-2229.12013>.
 37. Gilbert JA, Field D, Swift P, Newbold L, Oliver A, Smyth T, Somerfield PJ, Huse S, Joint I. 2009. The seasonal structure of microbial communities in the western English Channel. *Environ Microbiol* 11:3132–3139. <http://dx.doi.org/10.1111/j.1462-2920.2009.02017.x>.
 38. Gilbert JA, Steele JA, Caporaso JG, Steinbrück L, Reeder J, Temperton B, Huse S, McHardy AC, Knight R, Joint I, Somerfield P, Fuhrman JA, Field D. 2012. Defining seasonal marine microbial community dynamics. *ISME J* 6:298–308. <http://dx.doi.org/10.1038/ismej.2011.107>.
 39. Teeling H, Fuchs BM, Becher D, Klockow C, Gardebrecht A, Bennis CM, Kassabgy M, Huang S, Mann AJ, Waldmann J, Weber M, Klindworth A, Otto A, Lange J, Bernhardt J, Reinsch C, Hecker M, Peplies J, Bockelmann FD, Callies U, Gerdtts G, Wichels A, Wiltshire KH, Glöckner FO, Schweder T, Amann R. 2012. Substrate-controlled succession of marine bacterioplankton populations induced by a phytoplankton bloom. *Science* 336:608–611. <http://dx.doi.org/10.1126/science.1218344>.
 40. Galand PE, Potvin M, Casamayor EO, Lovejoy C. 2010. Hydrography shapes bacterial biogeography of the deep Arctic Ocean. *ISME J* 4:564–576. <http://dx.doi.org/10.1038/ismej.2009.134>.
 41. Schattnerhofer M, Fuchs BM, Amann R, Zubkov MV, Tarran GA, Pernthaler J. 2009. Latitudinal distribution of prokaryotic picoplankton populations in the Atlantic Ocean. *Environ Microbiol* 11:2078–2093. <http://dx.doi.org/10.1111/j.1462-2920.2009.01929.x>.
 42. Yin Q, Fu B, Li B, Shi X, Inagaki F, Zhang X-H. 2013. Spatial variations in microbial community composition in surface seawater from the ultratropical center to rim of the South Pacific Gyre. *PLoS One* 8:e55148. <http://dx.doi.org/10.1371/journal.pone.0055148>.
 43. Morris RM, Rappé MS, Connon SA, Vergin KL, Siebold WA, Carlson CA, Giovannoni SJ. 2002. SAR11 clade dominates ocean surface bacterioplankton communities. *Nature* 420:806–810. <http://dx.doi.org/10.1038/nature01240>.
 44. Rappé MS, Connon SA, Vergin KL, Giovannoni SJ. 2002. Cultivation of the ubiquitous SAR11 marine bacterioplankton clade. *Nature* 418:630–633. <http://dx.doi.org/10.1038/nature00917>.
 45. Giovannoni SJ, Tripp HJ, Givan S, Podar M, Vergin KL, Baptista D, Bibbs L, Eads J, Richardson TH, Noordewier M, Rappé MS, Short JM, Carrington JC, Mathur EJ. 2005. Genome streamlining in a cosmopolitan oceanic bacterium. *Science* 309:1242–1245. <http://dx.doi.org/10.1126/science.1114057>.
 46. Casey JR, Aucion JP, Goldberg SR, Lomas MW. 2013. Changes in partitioning of carbon amongst photosynthetic pico- and nano-plankton groups in the Sargasso Sea in response to changes in the North Atlantic Oscillation. *Deep Sea Res Part II Top Stud Oceanogr* 93:58–70. <http://dx.doi.org/10.1016/j.dsr2.2013.02.002>.
 47. Mella-Flores D, Mazard S, Humily F, Partensky F, Mahé F, Bariat L, Courties C, Marie D, Ras J, Mauriac R, Jeanthon C, Mahdi Bendif E, Ostrowski M, Scanlan DJ, Garczarek L. 2011. Is the distribution of *Prochlorococcus* and *Synechococcus* ecotypes in the Mediterranean Sea affected by global warming? *Biogeosciences* 8:2785–2804. <http://dx.doi.org/10.5194/bg-8-2785-2011>.
 48. Sintes E, Witte H, Stodderegger K, Steiner P, Herndl GJ. 2013. Temporal dynamics in the free-living bacterial community composition in the coastal North Sea. *FEMS Microbiol Ecol* 83:413–424. <http://dx.doi.org/10.1111/1574-6941.12003>.
 49. Varela MM, van Aken HM, Sintes E, Herndl GJ. 2008. Latitudinal trends of Crenarchaeota and Bacteria in the meso- and bathypelagic water masses of the eastern North Atlantic. *Environ Microbiol* 10:110–124. <http://dx.doi.org/10.1111/j.1462-2920.2007.01437.x>.
 50. De Corte D, Yokokawa T, Varela MM, Agogué H, Herndl GJ. 2009. Spatial distribution of Bacteria and Archaea and amoA gene copy numbers throughout the water column of the eastern Mediterranean Sea. *ISME J* 3:147–158. <http://dx.doi.org/10.1038/ismej.2008.94>.
 51. Weinbauer MG, Liu J, Motegi C, Maier C, Pedrotti ML, Dai M, Gattuso JP. 2013. Seasonal variability of microbial respiration and bacterial and archaeal community composition in the upper twilight zone. *Aquat Microb Ecol* 71:99–115. <http://dx.doi.org/10.3354/ame01666>.
 52. Piccini C, Conde D, Alonso C, Sommaruga R, Pernthaler J. 2006. Blooms of single bacterial species in a coastal lagoon of the southwestern Atlantic Ocean. *Appl Environ Microbiol* 72:6560–6568. <http://dx.doi.org/10.1128/AEM.01089-06>.
 53. Varela MM, van Aken HM, Herndl GJ. 2008. Abundance and activity of Chloroflexi-type SAR202 bacterioplankton in the meso- and bathypelagic waters of the (sub)tropical Atlantic. *Environ Microbiol* 10:1903–1911. <http://dx.doi.org/10.1111/j.1462-2920.2008.01627.x>.
 54. Vergin KL, Beszteri B, Monier A, Thrash JC, Temperton B, Treusch AH, Kilpert F, Worden AZ, Giovannoni SJ. 2013. High-resolution SAR11 ecotype dynamics at the Bermuda Atlantic time-series study site by phylogenetic placement of pyrosequences. *ISME J* 7:1322–1332. <http://dx.doi.org/10.1038/ismej.2013.32>.
 55. Stahl DA, Amann R. 1991. Development and application of nucleic acid probes, p 205–248. *In* Stackebrandt E, Goodfellow M (ed), *Nucleic acid techniques in bacterial systematics*. John Wiley & Sons, Ltd., Chichester, United Kingdom.
 56. Amann RI, Binder BJ, Olson RJ, Chisholm SW, Devereux R, Stahl DA. 1990. Combination of 16S rRNA-targeted oligonucleotide probes with flow cytometry for analyzing mixed microbial populations. *Appl Environ Microbiol* 56:1919–1925.
 57. Daims H, Brühl A, Amann R, Schleifer KH, Wagner M. 1999. The domain-specific probe EUB338 is insufficient for the detection of all Bacteria: development and evaluation of a more comprehensive probe set. *Syst Appl Microbiol* 22:434–444. [http://dx.doi.org/10.1016/S0723-2020\(99\)80053-8](http://dx.doi.org/10.1016/S0723-2020(99)80053-8).
 58. Wallner G, Amann R, Beisker W. 1993. Optimizing fluorescent in situ hybridization with rRNA-targeted oligonucleotide probes for flow cytometric identification of microorganisms. *Cytometry* 14:136–143. <http://dx.doi.org/10.1002/cyto.990140205>.
 59. Manz W, Amann R, Ludwig W, Vancanneyt M, Schleifer KH. 1996. Application of a suite of 16S rRNA-specific oligonucleotide probes designed to investigate bacteria of the phylum Cytophaga-Flavobacter-Bacteroides in the natural environment. *Microbiology* 142:1097–1106. <http://dx.doi.org/10.1099/13500872-142-5-1097>.
 60. Morris RM, Rappé MS, Urbach E, Connon SA, Giovannoni SJ. 2004. Prevalence of the Chloroflexi-related SAR202 bacterioplankton cluster throughout the mesopelagic zone and deep ocean. *Appl Environ Microbiol* 70:2836–2842. <http://dx.doi.org/10.1128/AEM.70.5.2836-2842.2004>.
 61. Schönhuber W, Zarda B, Eix S, Rippka R, Herdman M, Ludwig W, Amann R. 1999. In situ identification of cyanobacteria with horseradish peroxidase-labeled, rRNA-targeted oligonucleotide probes. *Appl Environ Microbiol* 65:1259–1267.
 62. Fuchs BM, Woebken D, Zubkov MV, Burkill P, Amann R. 2005. Molecular identification of picoplankton populations in contrasting waters of the Arabian Sea. *Aquat Microb Ecol* 39:145–157. <http://dx.doi.org/10.3354/ame039145>.
 63. Eilers H, Pernthaler J, Peplies J, Glöckner FO, Gerdtts G, Amann R. 2001. Isolation of novel pelagic bacteria from the German bight and their seasonal contributions to surface picoplankton. *Appl Environ Microbiol* 67:5134–5142. <http://dx.doi.org/10.1128/AEM.67.11.5134-5142.2001>.
 64. Manz W, Amann R, Ludwig W, Wagner M, Schleifer K-H. 1992. Phylogenetic oligonucleotide probes for the major subclasses of Proteobacteria: problems and solutions. *Syst Appl Microbiol* 15:593–600. [http://dx.doi.org/10.1016/S0723-2020\(11\)80121-9](http://dx.doi.org/10.1016/S0723-2020(11)80121-9).
 65. Zubkov MV, Fuchs BM, Burkill PH, Amann R. 2001. Comparison of cellular and biomass specific activities of dominant bacterioplankton groups in stratified waters of the Celtic Sea. *Appl Environ Microbiol* 67: 5210–5218. <http://dx.doi.org/10.1128/AEM.67.11.5210-5218.2001>.